
Effect of Averaging Timescale on a Forced Lorenz Model

Suneet Dwivedi^{1,2,3,*}, Ashok Kumar Mittal^{1,2,3} and Avinash Chandra Pandey^{1,2,3}

¹*M. N. Saha Centre of Space Studies, Institute of Interdisciplinary Studies
University of Allahabad, Allahabad*

²*K. Banerjee Centre of Atmospheric and Ocean Studies
Institute of Interdisciplinary Studies, University of Allahabad, Allahabad*

³*Department of Physics, University of Allahabad
Allahabad (UP), India Pin-211002*

[Original manuscript received 10 April 2006; in revised form 25 October 2006]

ABSTRACT *The effect of temporal averaging on the forced Lorenz model is studied. It is shown that the duration of temporal averaging affects the regime structure. When temporal averaging is increased beyond the fast timescale of the Lorenz model, regime splitting takes place. The increase in the predictability of the system with an increase in moving time average steps is quantified. Our findings from a conceptual forced Lorenz model are consistent with real world observations.*

RÉSUMÉ [Traduit par la rédaction] *On étudie l'effet du moyennage temporel sur le modèle de Lorenz forcé. On montre que l'étendue du moyennage dans le temps a un effet sur la structure du régime. Quand le moyennage temporel est augmenté au-delà de l'échelle de temps rapide du modèle de Lorenz, il se produit une séparation de régime. On quantifie l'augmentation de prévisibilité du système en fonction de l'augmentation des pas de moyennage temporel mobiles. Nos résultats à partir d'un modèle de Lorenz conceptuel forcé correspondent aux observations du monde réel.*

1 Introduction

Typically, weather and climate datasets consist of time- and space-averaged values of continuous variables. Many investigators have studied the influence of time averaging in weather and climate studies. Teng et al. (2004) studied the effects of different temporal averaging timescales on the regime structure of the extratropical northern hemisphere in reanalysis data and in a global climate model and showed that temporal averaging can significantly change the regime structure when the averaging timescale is considerably longer than the intrinsic regime residence time. They concluded that there is a need to consider carefully the averaging timescales used in diagnostic studies of the non-Gaussian structure of climate data. While some averaging is generally necessary to suppress noise, too much averaging can significantly change the structure of the atmospheric data.

Yuval and Hsieh (2002) demonstrated that non-linear empirical relations between different variables tend to become multivariate normal as the averaging duration increases.

Despite the fact that there is a theoretical limit of about two weeks beyond which it would be impossible to predict the state of the atmosphere (Lorenz, 1982), skilful longer-range predictions of seasonally averaged rainfall have been successfully made (Gowariker et al., 1991). The existence of lower boundary forcings such as sea surface temperature (SST) and averaging have been advanced as possible explanations for this increased predictability (Charney and Shukla, 1981; Shukla, 1981, 1998; Shukla and Paolino, 1983; Palmer et al., 1992).

According to Shukla and Fennessy (1988), the limit of deterministic predictability of about two weeks, based on classical predictability studies, does not apply to the predictability of the space-time averages, because the former refers to the predictability of the instantaneous flows whereas the latter refers to the average properties of the flow.

However, when available data is scarce, a problem with simple averaging is that it leads to a drastic reduction in the amount of data available for analysis. M step averaging of a

*Corresponding author's e-mail: dwivedisuneet@rediffmail.com

climate dataset of length N will reduce the size of the dataset to N/M . This problem may be overcome by using moving time averages because as well as having nearly the same gross features as simple time averaging, the size of the dataset remains nearly the same. This means that all the advantages of time averaging can be retained while the length of the available dataset (information) remains almost the same.

Palmer (1994) introduced a conceptual forced Lorenz model to explore the effects of lower boundary forcings such as SST on seasonally averaged rainfall. The ‘forcing’ term in Palmer’s model corresponds to the tropical Pacific SST anomaly and the two wings of the Lorenz butterfly represent the quiet and active monsoon periods. The forced Lorenz model, as a conceptual model of the atmosphere, has been the subject of several studies (Palmer, 1993, 1994, 1998; Corti et al., 1999; Pal and Shah, 1999; Mittal et al., 2003, 2005; Mehta et al., 2003; Yadav et al., 2005).

Pal and Shah (1999) presented some interesting results about sliding averages of the forced Lorenz model in order to explore the predictability of time averages beyond the predictability limit of instantaneous values. These results need to be explored further in a quantitative manner. In this paper we investigate how the largest Lyapunov exponent, information entropy and the autocorrelation function vary with the moving average time and with forcing. We have also applied non-linear principal component analysis (NLPCA) and calculated the fraction of explained variance (FEV) from the first non-linear mode.

It is also shown here that with an increase in moving average steps, the attractor shrinks. Therefore, the prediction error will become saturated near the overall size of the attractor (Kennel et al., 1994). The smaller the size of the attractor, the smaller the saturation error will be and therefore there will be greater predictability.

Section 2 briefly describes the basic concepts regarding these quantification measures. Section 3 describes the methodology and results.

2 Basic concepts

a Largest Lyapunov Exponent

The largest Lyapunov exponent is defined by

$$\lambda_1 = \lim_{n \rightarrow \infty} (1/n\tau) \sum_{k=1}^n \ln |d_k / d_{k-1}| \quad (1)$$

where d_0 and d_k represent, respectively, the distance between nearby trajectories in the phase space at the initial time and at time $k\tau$. The larger λ_1 is, the lower the predictability is. The Lyapunov exponent is a measure of the average rate at which nearby trajectories converge or diverge in the phase space i.e., it describes the average rate at which the predictability is lost. The Lyapunov exponent quantifies time-averaged predictability by measuring the mean rate of growth of small perturbations on an attractor. The Lyapunov exponent from meteorological time series and from low order models has been estimated by several authors (Zeng et al., 1992; Nese and Dutton, 1993; Yoden and Nomura, 1993).

b Entropy

Shannon entropy, the amount of information required to specify the state of the system (Sprott, 2003), is defined as

$$S_E = -\sum_i P_i \log P_i \quad (2)$$

where P_i is the probability of the state i .

If there are N points on the attractor with N_i of them in a cube i then $P_i = N_i/N$. For a periodic system, entropy is always zero and for a chaotic system it has a positive (large) value. As entropy decreases, the predictability of the system increases.

The inverse of entropy estimates the time in which predictability is lost. Entropy has been used as a statistical measure in predictability studies of atmosphere and climate (Carnevale and Vallis, 1983; Kleeman, 2002; Schneider and Griffies, 1999; DelSole, 2004).

c Non-linear Principal Component Analysis (NLPCA)

Kramer (1991) proposed a neural network-based NLPCA technique to obtain a low-dimensional approximation of the given dataset. Principal component analysis only allows linear mappings between x (the dataset) and the principal component; NLPCA allows non-linear mappings. An auto-associative feed forward neural network, which contains three hidden layers of neurons between the input and output layers of variables is used to perform NLPCA. The NLPCA technique has been widely used in meteorology to derive the dominant patterns of variability (Hsieh, 2004 and references therein).

d Autocorrelation Function

The autocorrelation function $G(k)$, defined as

$$G(k) = \frac{\sum_{n=1}^{N-k} (X_n - \langle X \rangle)(X_{n+k} - \langle X \rangle)}{\sum_{n=1}^{N-k} (X_n - \langle X \rangle)^2}, \quad (3)$$

measures how strongly, on average, each data point is correlated with one k steps away. The value of k at which $G(k)$ falls to $1/e \approx 37\%$ is called the correlation time, τ_c . The autocorrelation function is symmetric about $k = 0$ and so the quantity, $2\tau_c$, measures how much memory the system has. The reciprocal of this quantity, $0.5/\tau_c$, gives an estimate of the average rate at which predictability is lost (Sprott, 2003).

3 Methodology and discussion

Palmer (1994) modified the Lorenz model (Lorenz, 1963) to

$$\begin{aligned} dx/dt &= -ax + ay + F_x \\ dy/dt &= -xz + rx - y + F_y \\ dz/dt &= xy - bz + F_z \end{aligned} \quad (4)$$

where $a = 10$, $b = 8/3$ and $r = 28$. This forced Lorenz model has been investigated for $F_x = aF$, $F_y = -F$, $F_z = 0$ as this case

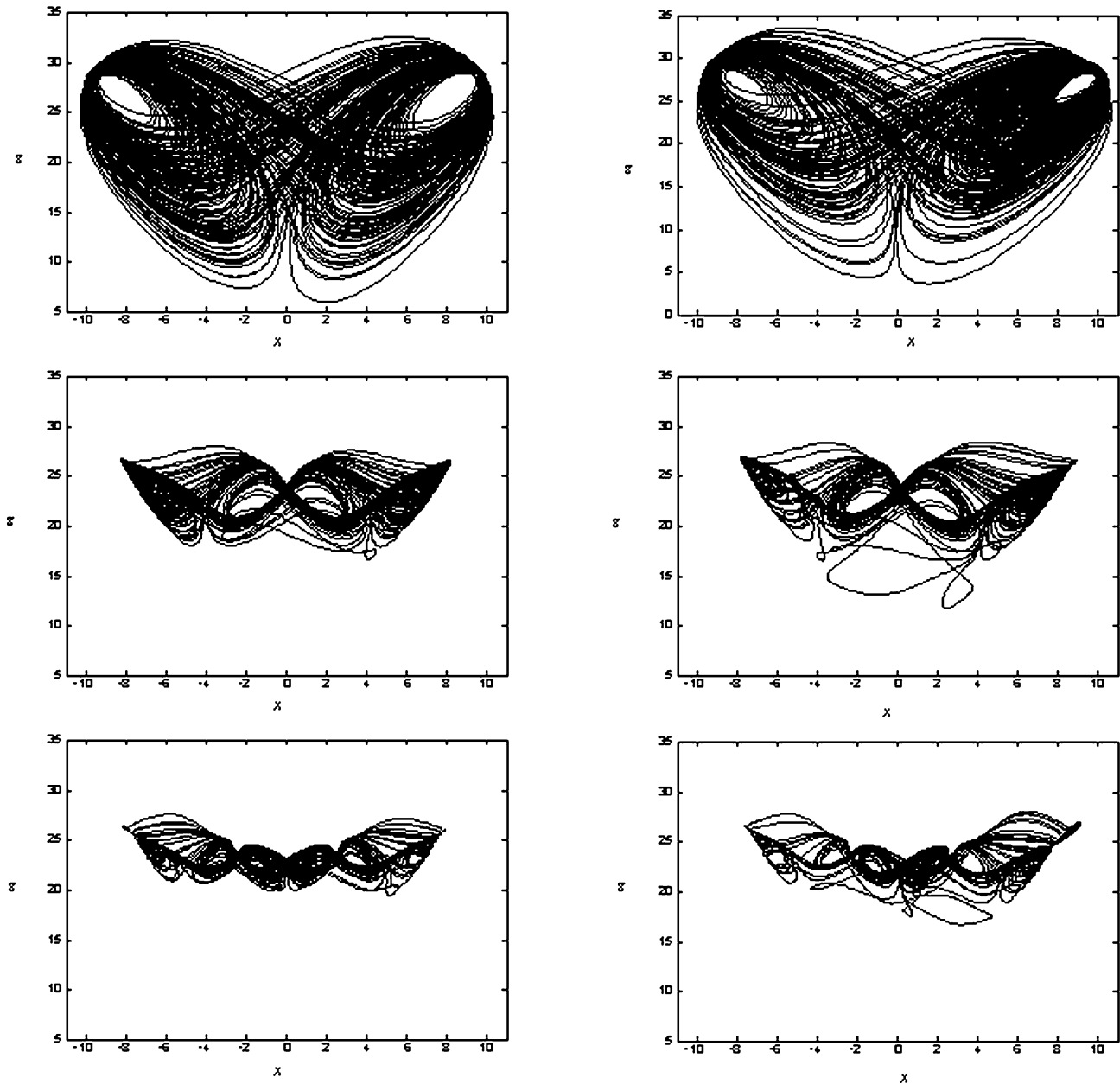


Fig. 1 Change in the shape of the Lorenz attractor for sliding average time steps 40, 120, 200 respectively (from top to bottom) and for fixed forcing values $F_x = aF$, $F_y = -F$ for $F = 0$ (left panels) and $F = 1.5$ (right panels).

provides a simplified mathematical analysis (Mittal et al., 2003, 2005).

A sliding average applied to the output from the forced Lorenz model reveals interesting results when we vary the averaging steps and apply forcing at the same time. Figure 1 shows the changes in the shape of the Lorenz attractor for $F = 0$ and $F = 1.5$ when the number of time steps is increased. If F is greater than a critical value, F_c (nearly equal to 1.65), the attractor becomes a fixed point (Mittal et al., 2005). We have chosen $F = 1.5$, a value slightly less than F_c , in order to have a pronounced forcing effect while retaining the bimodal character of the Lorenz model. We observe that there is little forcing effect on the shape of the attractors, however, as

shown in Mittal et al. (2005); the probability of occupancy of the two wings of the unaveraged Lorenz attractor changes with forcing F . Figure 2 shows the probability, p_+ , of occupancy of the positive regime as a function of F . In this figure the dots indicate the average value of p_+ obtained from an ensemble of ten randomly chosen initial conditions. The error bars indicate the standard deviation of these values.

With an increase in the number of averaging steps the attractor splits into more regimes and occupies a smaller region in the phase space. This suggests an increase in predictability with both forcing and moving average steps, in one case due to a change in the probability distribution function and in the other due to the shrinking of the attractor. We have

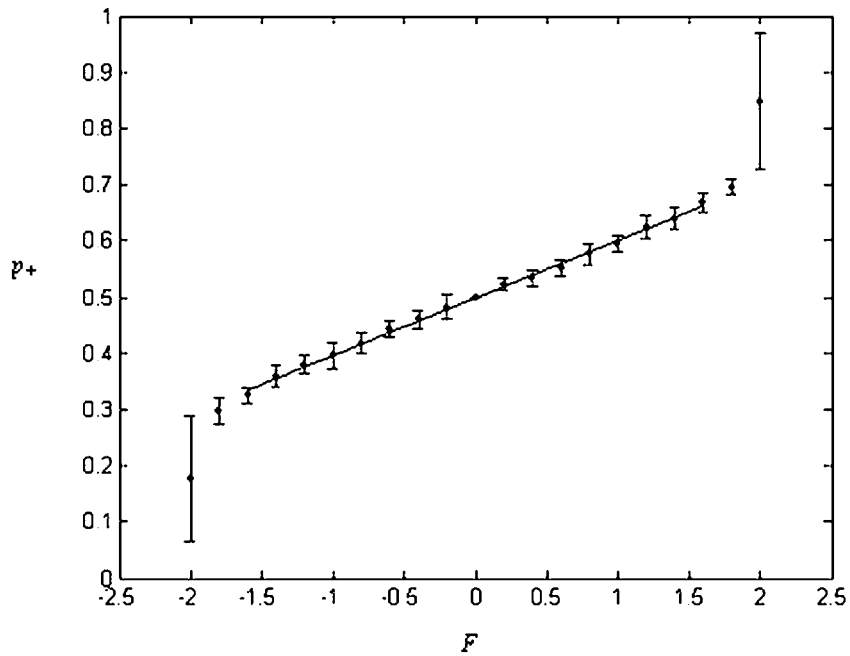


Fig. 2 Plot of probability (p_+) in $x > 0$ half space of the forced Lorenz model versus the forcing parameter F ($F_x = aF$, $F_y = -F$).

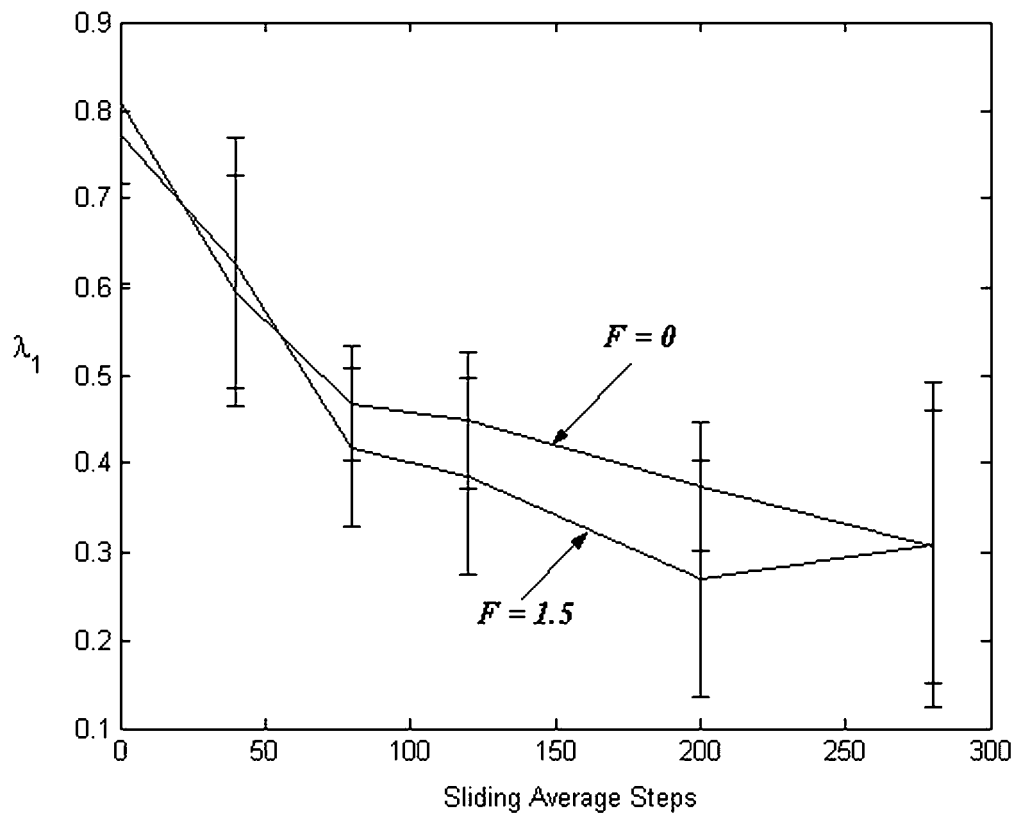


Fig. 3 Plot of largest Lyapunov exponent (λ_1) versus moving (sliding) average time steps for a fixed value of forcing $F_x = aF$, $F_y = -F$ for $F = 0$ and $F = 1.5$.

applied the techniques of non-linear dynamics, namely, the largest Lyapunov exponent, Shannon entropy, NLPCA and the autocorrelation function in order to explore the changes in predictability. These quantities provide useful information about the phase space structure and predictability characteris-

tics of attractors. We find that the effect of forcing on predictability is small compared to that due to averaging.

The largest Lyapunov exponent (λ_1) of the time series of variable x obtained by numerical integration of Eq. (4) for a time step of 0.01 was determined using Wolf et al.'s (1985)

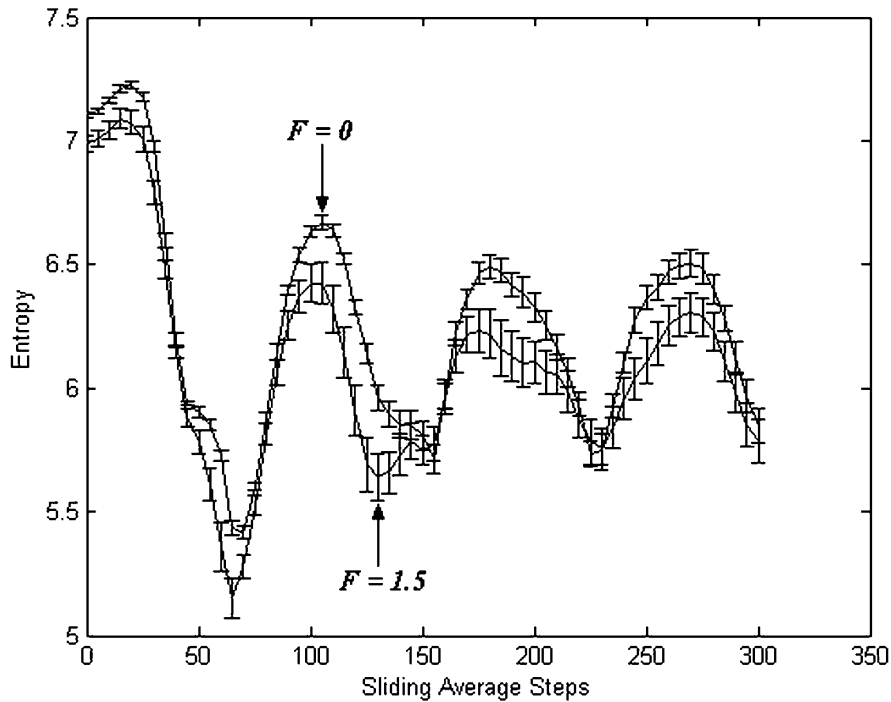


Fig. 4 Plot of Shannon information entropy of the forced Lorenz attractor versus moving (sliding) average time steps for fixed values of forcing $F_x = aF$, $F_y = -F$; $F = 0$ and $F = 1.5$.

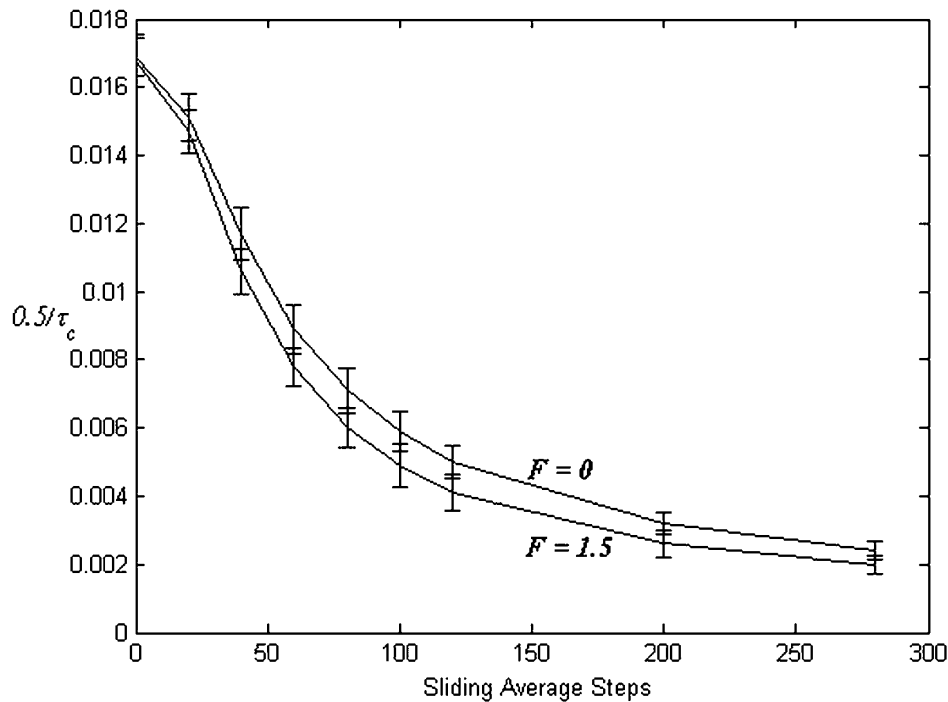


Fig. 5 Plot of loss in predictability ($0.5/\tau_c$) versus the moving average steps for $F = 0$ and $F = 1.5$.

algorithm as a function of averaging steps for fixed forcing values $F_x = aF$, $F_y = -F$ for $F = 0$ and $F = 1.5$, respectively. λ_1 as a function of averaging steps for fixed forcing values is calculated for ten different initial conditions. The ensemble averaged λ_1 with error bars (standard deviation of the ensemble mean) is plotted as a function of averaging steps for $F = 0$

and 1.5 in Fig. 3. It seems that the effect of forcing on the largest Lyapunov exponent is small.

Shannon entropy was computed using the technique discussed in Section 2b. The ensemble average over ten initial conditions is shown in Fig. 4 as a function of averaging steps for fixed forcing values $F = 0$ and 1.5. The wave structure

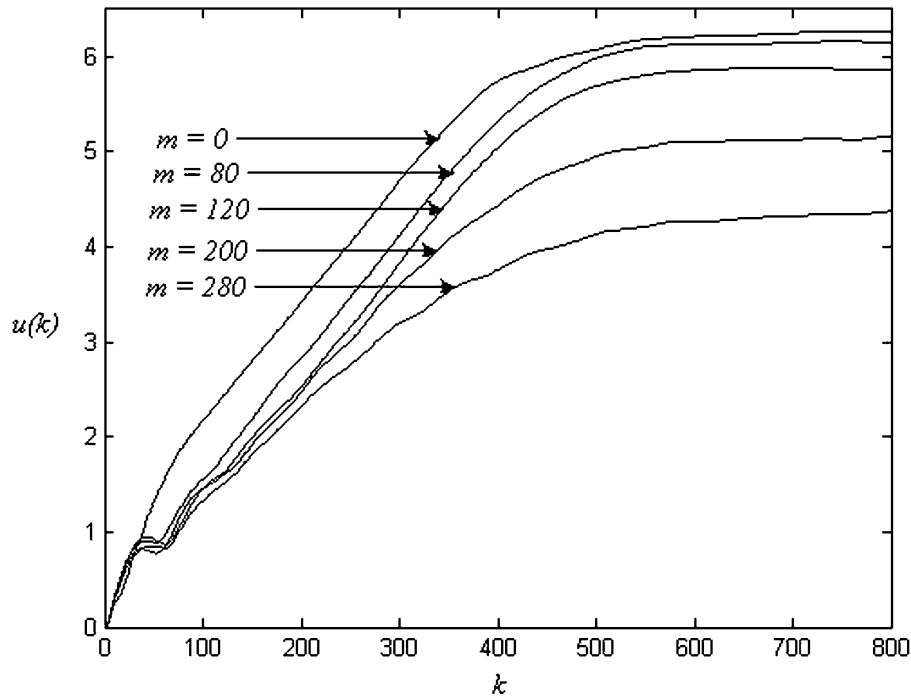


Fig. 6 Plot of the unpredictability measure $u(k)$ versus the prediction time steps, k , for different moving average steps, m .

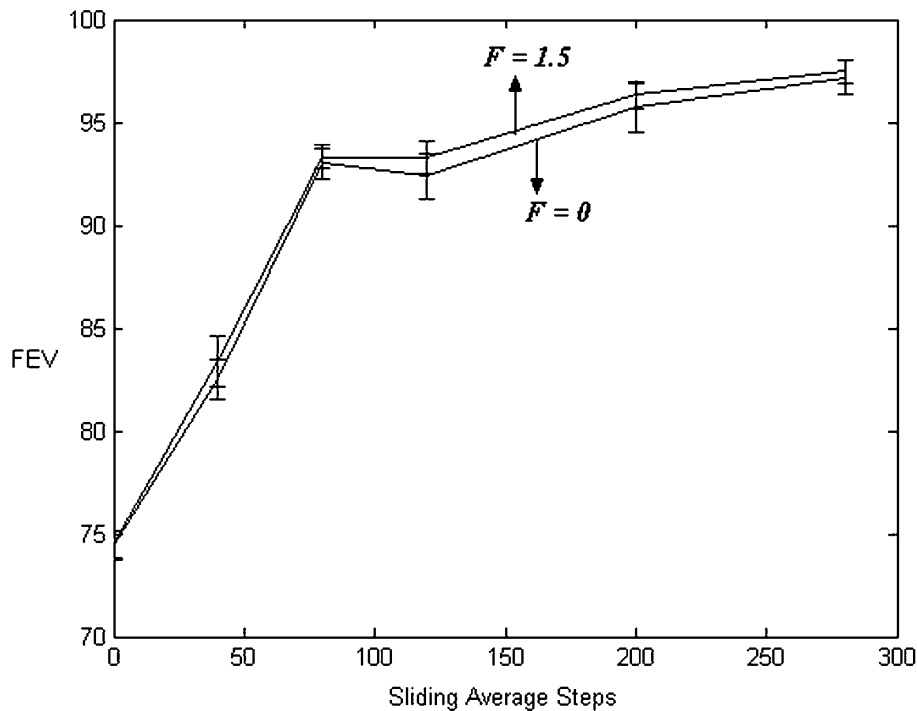


Fig. 7 Plot of the fraction of explained variance (FEV) of the first non-linear principal component of the forced Lorenz attractor versus the moving average time steps for fixed values of forcing, $F_x = aF$, $F_y = -F$ for $F = 0$ and $F = 1.5$.

found in Fig. 4 is quite intriguing. The period of the wave is about 80 time steps. The Lorenz model has two characteristic timescales: (i) a timescale corresponding to a typical cycle about one of the unstable fixed points (50–70 time steps) and, (ii) a regime residency timescale (about 160 time steps). The wave timescale is slightly greater than the cycle timescale.

With an increase in moving average steps, the correlation time, τ_c , increases and therefore predictability increases. The loss of predictability ($0.5/\tau_c$) ensemble averaged over ten initial conditions as a function of moving average steps is shown in Fig. 5 for $F = 0$ and 1.5.

Let the true and measured states of a dynamical system at $t = 0$ be denoted by x_0 and x'_0 respectively. Then $\epsilon_0 = \|x_0 - x'_0\|$

is the initial error. Let the true and predicted states at time $t_k = k\tau$ using the dynamical evolution law be x_k and x'_k respectively. The error in prediction will be $\epsilon_k = \|x_k - x'_k\|$ and it clearly depends on x_0 , ϵ_0 and the dynamical evolution law. An appropriate measure of the unpredictability of the state x_0 at time t_k will be $u(x_0, k) = \log_2(\epsilon_k/\epsilon_0)$. This value averaged over the different initial states, x_0 , of the attractor gives a measure of the unpredictability, $u(k)$, of the system k time steps in advance. The smaller the attractor, the smaller is the expected value of ϵ_k and therefore of $u(k)$, and the greater the predictability.

We used the algorithm given in Parlitz (1998) to estimate the unpredictability, $u(k)$, of the moving averaged Lorenz system for different averaging time steps, m . The results are summarized in Fig. 6 which shows that the unpredictability measure, $u(k)$, decreases with increasing m . Thus, increasing the length of the averaging window leads to greater predictability due to a smaller attractor size.

NLPCA determines a non-linear mapping from the data to a low-dimensional manifold embedded in the data space, so as to minimize the mean square error (MSE) between the data and its image. In this way NLPCA provides a low-dimensional approximation to the given data. A measure of the validity of this approximation is the FEV. It can be made arbitrarily close to its maximum value of unity by the appropriate choice of a neural network. However, such a network will only be useful if it gives a good representation for data that were not used in training the network. If this is not the case, the network is said to be overfitted.

To avoid the problem of overfitting, some of the data are used for optimizing the weights of the neural network and the remaining data are used for testing this network. During the optimization process it is common to monitor the MSE for the training data and for the test data separately. As the number of iterations of the optimization algorithm increases, the MSE calculated for the training data decreases; however, beyond a certain number of iterations the MSE for the test data would begin to increase, indicating the start of overfitting and hence the appropriate time to stop the optimization process. If the MSE for the test data is greater than that for the training data, the neural network is not included in the ensemble of neural networks from which the best neural network is chosen. The best neural network is the one that minimizes the MSE for all the data.

We used the NLPCA technique of Hsieh (2004), which is based on Kramer (1991) and obtained the FEV of the forced Lorenz model for fixed forcing values $F = 0$ and $F = 1.5$ with an increase in averaging steps. This is shown in Fig. 7, where with the increase in the number of averaging steps, the FEV of the first non-linear principal component mode increases from 75% (0 averaging steps) to nearly 97% (280 averaging steps) for $F = 0$, which is further increased in the case of $F = 1.5$. An increase in FEV means that more variance is captured in a single non-linear mode suggesting that the system is easier to predict with an increase in averaging steps and an increase in forcing.

It should be noted that the FEV statistic from NLPCA as a measure of predictability is of a different nature than predictability measures based on error growth rate. The latter assume that the evolution law of the system is perfect and the unpredictability arises due to errors in the initial conditions. The former measures the extent to which it is possible to model the observed time series by a deterministic system. The evolution of any meteorological variable is governed by a large number of intractable influences. However, in some cases the evolution may be primarily governed by a few causes, the intractable influences leading to stochastic variability. In such cases a few non-linear modes may be expected to explain a large fraction of the variance and one may model the system by a deterministic dynamical system representing these few modes. Let $x(t)$ denote the state of the entire system at time t and $x_p(t)$ be its projection on these few modes. Given a sufficiently long series of values of x_p , it is possible to predict values using the algorithm of Farmer and Sidorowich (1987). The lower the dimension of x_p , the better this algorithm works and the greater the prediction time. Therefore, x_p may be regarded as a predictable part of x and the fraction of variance it explains as a measure of predictability.

One may treat the time series obtained by adding random noise in the range $[-1, 1]$ to the output from a Lorenz model, as a conceptual representation of an experimentally measured time series from an unknown dynamical system and find that it can be modelled by a single non-linear mode, which explains a large fraction of the variability of the output. The larger the FEV explained by this mode, the better the predictability.

A trajectory $x(t_n)$, $t_n = n\tau$, $n = 1, 2, \dots, N + k$, $N = 1000$, $k = 2, 4, 6, 8, 10$ on a noisy Lorenz attractor, was projected to $x_p(t_n)$ on the dominant non-linear principal component mode by using an auto-associative feed forward neural network. For this projected trajectory, using the technique of Farmer and Sidorowich (1987), predictions were made with a forecast lead time, $k\tau$, and the predicted trajectory denoted by $x_{pp}(t_{n+k})$, $n = 1, 2, \dots, N$. A measure of the prediction error at lead time $k\tau$ is given by

$$e(k) = \left[\frac{1}{N} \sum_{n=1}^N \{x_{pp}(t_{n+k}) - x(t_{n+k})\}^2 \right]^{1/2}.$$

This error is normalized by the standard deviation of $x(t)$ to give the normalized prediction error, $E(k)$.

A moving time-averaged series, $x^{<m>}(t_n)$, with an averaging window of length m was obtained from the output of the Lorenz model. This was projected to $x_p^{<m>}(t_n)$ on the dominant non-linear principal component mode and predictions were made from this projected series by the Farmer and Sidorowich (1987) algorithm. The prediction error,

$$e^{<m>}(k) = \left[\frac{1}{N} \sum_{n=1}^N \{x_{pp}^{<m>}(t_{n+k}) - x^{<m>}(t_{n+k})\}^2 \right]^{1/2}$$

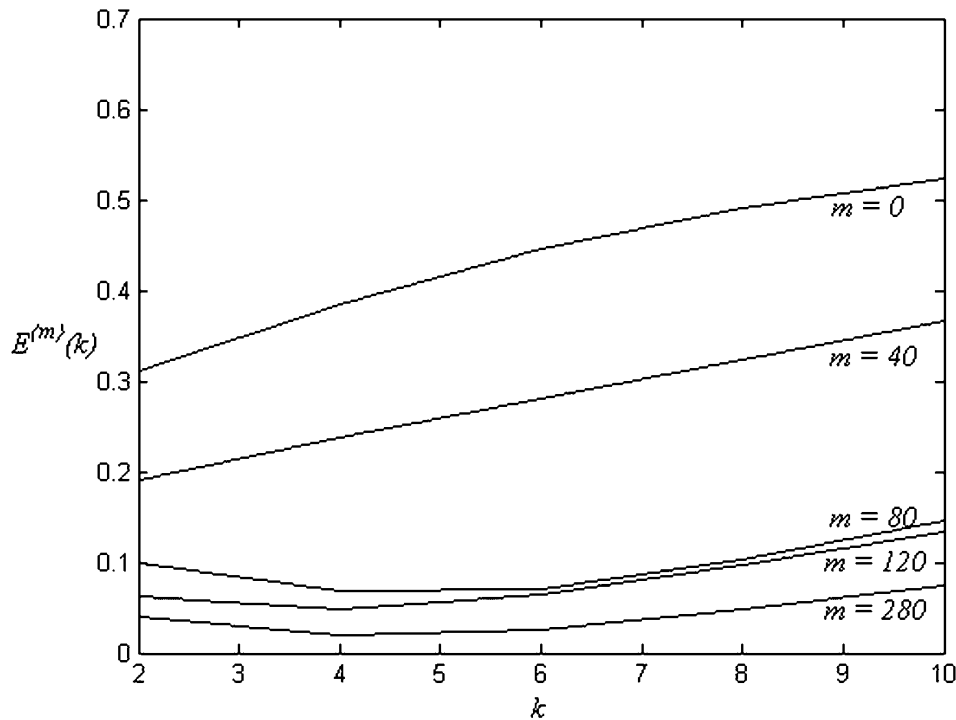


Fig. 8 Plot of normalized prediction error $E^{<m>(k)}$ as a function of prediction time steps, k , for different moving average steps, m .

was normalized by the standard deviation of $x^{<m>(t)}$ to obtain the normalized prediction error, $E^{<m>(k)}$. Plots of $E^{<m>(k)}$ as a function of k for different values of m are shown in Fig. 8. It is clear from this figure that as m increases, the prediction error decreases and therefore predictability increases.

It may be mentioned that there is another sense in which FEV is connected to predictability. Larger FEV means greater correlation between the different variables of the system, so that measurement of some of the variables at some time may be used to predict the values of the remainder of the variables at the same time.

We find that as the length of the moving average window is increased there is a decrease in the largest Lyapunov exponent, the Shannon entropy and the unpredictability measure and an increase in the correlation time and FEV of the first nonlinear principal component of the moving time-averaged forced Lorenz model. Each of the quantitative measures investigated suggests an increase in predictability with an increase in the moving average step size as well as with an increase in forcing.

4 Conclusions

With an increase in the sliding time-averaged step size as well as with an increase in forcing, the attractor splits into more regimes and occupies a smaller region in the phase space. The smaller the size of the attractor, the smaller the saturation error (Kennel et al., 1994) and therefore the greater the predictability.

The change in predictability with averaging time step duration and forcing has been quantified by calculating the largest

Lyapunov exponent, Shannon's entropy, the FEV of the first non-linear principal component, and the autocorrelation function (loss in prediction) of the moving averaged forced Lorenz model. All the calculations suggest that predictability increases with the increase in moving average time steps, and it is further increased when forcing is applied, however, the effect of forcing is small compared to the effect of averaging. The increase in predictability observed here is in agreement with the suggestions of Shukla (1984) and Shukla and Fennessy (1988) that including the effects of the boundary conditions at the Earth's surface has the potential to enhance further the predictability of monthly and seasonal averages.

Unit non-dimensional time in the Lorenz model corresponds to about 10 days for the atmosphere (Palmer, 1993). Thus, in our simulation with a time step of 0.01, ten time steps correspond to one day. A typical cycle (fast timescale) in the Lorenz model contains about 50 time steps in our simulation, corresponding to about 5 days for the atmosphere. We found that as temporal averaging is increased beyond the fast timescale, the attractor splits into more regimes. This is analogous to the findings of Teng et al. (2004) that temporal averaging duration affects the regime structure for timescales longer than the intrinsic regime occupation timescale. However, it should be noted that in our study, regime splitting takes place for moving average timescales greater than the fast timescale, which is about one-third of the average regime residency time, but both studies demonstrate changes in the regime structure of the dataset with the averaging timescale. Our studies thus strengthen the significance of the forced Lorenz model as a conceptual model of the atmosphere.

Moving time averages may be used in place of time averaging in climate diagnostic studies because it keeps the size of the dataset almost the same while providing increased predictability. Meteorological data are typically the result of contributions from processes taking place on several timescales. Moving time averages suppress phenomena having timescales less than the averaging time. Therefore, the averaging time should not exceed the timescale of the physical process that is of interest. By choosing different averaging times, one can explore the structure of the data on different timescales.

This can help to reveal physical processes that take place on different timescales.

Acknowledgements

The authors would like to thank the Indian Space Research Organization (ISRO) and the National Centre of Antarctic and Ocean Research (NCAOR), Goa/Department of Ocean Development (DOD) for financial assistance in the form of a project.

References

- CARNEVALE, G. F. and G. K. VALLIS. 1983. Applications of entropy to predictability theory. *In: Am. Inst. Physics Proceedings, The Predictability of Fluid Motions*, G. Holloway and B. West (Eds), pp. 577-593.
- CHARNEY, J. G. and J. SHUKLA. 1981. Predictability of monsoons. *Monsoon Dynamics*, Sir J. Lighthill and R. P. Pearce (Eds), Cambridge Univ. Press, pp. 99-109.
- CORTI, S.; F. MOLteni and T. N. PALMER. 1999. Signature of recent climate change in frequencies of natural atmospheric circulation regimes. *Nature*, **398**: 799-802.
- DELSOLE, T. 2004. Predictability and information theory. Part I: Measures of predictability. *J. Atmos. Sci.* **61**:2425-2440.
- FARMER, J. D. and J. J. SIDOROWICH. 1987. Predicting chaotic time series. *Phys. Rev. Lett.* **59**: 845-848.
- GOWARIKER, V.; V. THAPLIYAL, S. M. KULSHESHTRA, G. S. MANDAL, N. ROY and D. R. SIKKA. 1991. A power regression model for long range forecast of southwest monsoon rainfall over India. *Mausam*, **42**: 125-130.
- HSIEH, W. W. 2004. Nonlinear multivariate and time series analysis by neural network methods. *Rev. Geophys.* **42**: RG1003 1-25. doi: 10.1029/2002RG000112.
- KENNEL, M. B.; H. D. I. ABARBANEL and J. J. SIDOROWICH. 1994. Prediction errors and local Lyapunov exponents, arXiv: chao-dyn/9403001 v1, 1-11.
- KLEEMAN, R. 2002. Measuring dynamical prediction utility using relative entropy. *J. Atmos. Sci.* **59**: 2057-2072.
- KRAMER, M. A. 1991. Nonlinear principal component analysis using autoassociative neural networks. *AICHE J.* **37**: 233-243.
- LORENZ, E. N. 1963. Deterministic non-periodic flow. *J. Atmos. Sci.* **20**: 130-141.
- LORENZ, E. N. 1982. Atmospheric predictability experiments with a large numerical model. *Tellus*, **43**: 505-513.
- MEHTA, M.; A. K. MITTAL and S. DWIVEDI. 2003. The double-cusp map for the forced Lorenz system. *Int. J. Bifur. Chaos*. **13**: 3029-3035.
- MITTAL, A. K.; S. DWIVEDI and A. C. PANDEY. 2003. A study of the forced Lorenz model of relevance to monsoon predictability. *Ind. J. Radio Space Phys.* **32**: 209-216.
- MITTAL, A. K.; S. DWIVEDI and A. C. PANDEY. 2005. Bifurcation analysis of a paradigmatic model of monsoon prediction. *Nonlinear Proc. Geophys.* **12**: 707-715.
- NESE, J. M. and J. A. DUTTON. 1993. Quantifying predictability variations in a low-order ocean-atmosphere model: A dynamical systems approach. *J. Clim.* **6**: 185-204.
- PAL, P. K. and S. SHAH. 1999. Feasibility study of extended range atmospheric prediction through time average Lorenz attractor. *Ind. J. Radio Space Phys.* **28**: 271-276.
- PALMER, T. N. 1993. Extended-range atmospheric prediction and the Lorenz model. *Bull. Am. Meteorol. Soc.* **74**: 49-66.
- PALMER, T. N. 1994. Chaos and predictability in forecasting the monsoons. *Proc. Ind. Natn. Sci. Acad.* **60 A**: 57-66.
- PALMER, T. N. 1998. A nonlinear dynamical perspective on climate Prediction. *J. Clim.* **12**: 575-591.
- PALMER, T. N.; C. BRANKOVIC, P. VITERBO and M. J. MILLER. 1992. Modeling interannual variations of summer monsoons. *J. Clim.* **5**: 399-417.
- PARLITZ, U. 1998. Nonlinear time-series analysis. *In: Nonlinear modeling-advanced black-box techniques*. J. A. K. Suykens and J. Vandewalle (Eds) Kluwer Academic Publishers, pp. 209-239.
- SCHNEIDER, T. and S. M. GRIFFIES. 1999. A conceptual framework for predictability studies. *J. Clim.* **12**: 3133-3155.
- SHUKLA, J. 1981. Dynamical predictability of monthly means. *J. Atmos. Sci.* **38**: 2547-2572.
- SHUKLA, J. 1984. Predictability of time averages: Part II, The influence of the boundary forcings. *In: Problems and prospects in long and medium range weather forecasting*. D. M. Burridge and E. Kallen (Eds) Springer Verlag, pp. 155-206.
- SHUKLA, J. 1998. Predictability in the midst of chaos: A scientific basis for climate forecasting. *Science*, **282**: 728-731.
- SHUKLA, J. and D. PAOLINO. 1983. The Southern Oscillation and long range forecasting of the summer monsoon rainfall over India. *Mon. Weather Rev.* **111**: 1830-1837.
- SHUKLA, J. and M. J. FENNESSY. 1988. Prediction of time mean atmospheric circulation and rainfall: Influence of the Pacific sea surface temperature anomaly. *J. Atmos. Sci.* **45**: 9-28.
- SPROTT, J. C. 2003. Chaos and time series analysis. Oxford University Press, New York. 507 pp.
- TENG, Q.; A. H. MONAHAN and J. C. FYFE. 2004. Effects of time averaging on climate regimes. *Geophys. Res. Lett.* **31**: doi: 10.1029/2004GL020840.
- WOLF, A.; J. SWIFT, H. SWINNEY and J. VASTANO. 1985. Determining Lyapunov exponents from a time series. *Physica D*, **16**: 285-317.
- YADAV, R. S.; S. DWIVEDI and A. K. MITTAL. 2005. Prediction rules for regime changes and length in new regime of the Lorenz's model. *J. Atmos. Sci.* **62**: 2316-2321.
- YODEN, S. and M. NOMURA. 1993. Finite-time Lyapunov stability analysis and its application to atmospheric predictability. *J. Atmos. Sci.* **50**: 1531-1543.
- YUVAL and W. W. HSIEH. 2002. The impact of time averaging on the detectability of nonlinear empirical relations. *Q. J. R. Meteorol. Soc.* **128**: 1609-1622.
- ZENG, X.; R. A. PIELKE and R. EYKHOLT. 1992. Estimate of the fractal dimension and predictability of the atmosphere. *J. Atmos. Sci.* **49**: 649-659.